

This article was downloaded by:

On: 25 January 2011

Access details: *Access Details: Free Access*

Publisher *Taylor & Francis*

Informa Ltd Registered in England and Wales Registered Number: 1072954 Registered office: Mortimer House, 37-41 Mortimer Street, London W1T 3JH, UK



## Separation Science and Technology

Publication details, including instructions for authors and subscription information:

<http://www.informaworld.com/smpp/title~content=t713708471>

### Numerical Simulation of Solute Dispersion in Laminar Tube Flow

K. P. Mayock<sup>a</sup>; J. M. Tarbell<sup>a</sup>; J. L. Duda<sup>a</sup>

<sup>a</sup> DEPARTMENT OF CHEMICAL ENGINEERING, PENNSYLVANIA STATE UNIVERSITY  
UNIVERSITY, PARK, PENNSYLVANIA

**To cite this Article** Mayock, K. P. , Tarbell, J. M. and Duda, J. L.(1980) 'Numerical Simulation of Solute Dispersion in Laminar Tube Flow', *Separation Science and Technology*, 15: 6, 1285 – 1296

**To link to this Article:** DOI: 10.1080/01496398008068505

**URL:** <http://dx.doi.org/10.1080/01496398008068505>

## PLEASE SCROLL DOWN FOR ARTICLE

Full terms and conditions of use: <http://www.informaworld.com/terms-and-conditions-of-access.pdf>

This article may be used for research, teaching and private study purposes. Any substantial or systematic reproduction, re-distribution, re-selling, loan or sub-licensing, systematic supply or distribution in any form to anyone is expressly forbidden.

The publisher does not give any warranty express or implied or make any representation that the contents will be complete or accurate or up to date. The accuracy of any instructions, formulae and drug doses should be independently verified with primary sources. The publisher shall not be liable for any loss, actions, claims, proceedings, demand or costs or damages whatsoever or howsoever caused arising directly or indirectly in connection with or arising out of the use of this material.

## Numerical Simulation of Solute Dispersion in Laminar Tube Flow

K. P. MAYOCK, J. M. TARBELL, and J. L. DUDA

DEPARTMENT OF CHEMICAL ENGINEERING  
PENNSYLVANIA STATE UNIVERSITY  
UNIVERSITY PARK, PENNSYLVANIA 16802

### Abstract

The dispersion of a solute slug in laminar tube flow has been simulated by a numerical method (the Flux Corrected Transport Algorithm) for a set of tube lengths embracing the pure convection through Taylor dispersion regimes. The results reveal unexpected double peak breakthrough curves for tubes of intermediate length. Experimental evidence of double peaks which qualitatively confirms the simulations is discussed.

### INTRODUCTION

Dispersion of a solute slug by a fluid being convected in laminar flow through a straight tube of circular cross section was first analyzed theoretically by Taylor (1) who solved for the area averaged concentration in the asymptotic case of long tubes at high Péclet number. Aris (2) also solved the long tube problem, but managed to relax the high Péclet number restriction. Gill and Sankarasubramanian (3) developed a more general dispersion theory which, in its usual truncated form, also applies to long tubes, although the tubes need not be so long as those of Taylor and Aris. The truncated dispersion theory of Gill and Sankarasubramanian certainly does not describe dispersion in short tubes [see Jayaraj and Subramanian (4) and Fife and Nicholes (5) for discussions of this point]. The breakthrough curves predicted by these long tube solutions are all characterized by smooth single peaks.

For short tubes the pure convection solution [see Taylor (1)] describes limiting behavior, and Lighthill's (6) solution describes asymptotic behavior near the pure convection limit. The short-tube breakthrough

curves are characterized by sharp single peaks with long tails. Lighthill indicates that his solution applies when  $t^* (= t/(R^2/D)) < 0.1$ , while Taylor's solution applies when  $t^* > 0.5$ .

In this paper we develop numerical solutions of the slug dispersion problem and monitor the breakthrough curves from the pure convection to the Taylor dispersion limits. In the process we uncover some rather unexpected double peak breakthrough curves for tubes of intermediate length. It should be noted that previous numerical solutions of the dispersion problem (7, 8) have not revealed the double peak behavior.

### THE DISPERSION MODEL

The dispersion of a solute by a fluid in fully developed, steady, laminar flow through a straight tube of circular cross section is modeled by the convective-diffusion equation

$$\frac{\partial c}{\partial t} + u_0 \left[ 1 - \frac{r^2}{R^2} \right] \frac{\partial c}{\partial Z} = D \left[ \frac{\partial^2 c}{\partial r^2} + \frac{1}{r} \frac{\partial c}{\partial r} \right] \quad (1)$$

in which the molecular diffusion coefficient ( $D$ ) is assumed constant and axial molecular diffusion is presumed negligible [cf. Taylor (1)]. The conditions to be imposed on the solution of Eq. (1) are

$$\begin{aligned} \frac{\partial c}{\partial r}(t, Z, 0) &= \frac{\partial c}{\partial r}(t, Z, R) = 0 \\ c(0, Z, r) &= c_0 \quad (0 \leq Z \leq Z_s) \\ &= 0 \quad (Z < 0, Z > Z_s) \end{aligned} \quad (2)$$

which describe a tube of fluid initially containing a uniform, axisymmetric slug of solute of length  $Z_s$  and concentration  $c_0$  emanating from an injection point ( $Z = 0$ ).

Introduction of the scaled variables

$$c^* = c/c_0, \quad r^* = r/R, \quad Z^* = Z/(R^2 u_0/D), \quad t^* = t/(R^2/D)$$

into Eq. (1) and Conditions (2) leads to the dimensionless dispersion model

$$\frac{\partial c^*}{\partial t^*} + (1 - r^{*2}) \frac{\partial c^*}{\partial Z^*} = \frac{\partial^2 c^*}{\partial r^{*2}} + \frac{1}{r^*} \frac{\partial c^*}{\partial r^*} \quad (3)$$

$$\begin{aligned} \frac{\partial c^*}{\partial r^*}(t^*, Z^*, 0) &= \frac{\partial c^*}{\partial r^*}(t^*, Z^*, 1) = 0 \\ c^*(0, Z^*, r^*) &= 1 \quad (0 \leq Z^* \leq Z_s^*) \\ &= 0 \quad (Z^* < 0, Z^* > Z_s^*) \end{aligned} \quad (4)$$

The area averaged mean concentration

$$c_m^*(t^*, Z^*) = 2 \int_0^1 c^* r^* dr^* \quad (5)$$

which is the concentration usually associated with dispersion theories, will be employed in presenting solutions of the dispersion model.

## NUMERICAL METHODS

Accurate numerical solutions of the slug dispersion problem for short times are difficult to obtain because the sharp axial concentration gradient induces *numerical dispersion* [*artificial viscosity* (9)] which masks the real dispersion. This phenomenon is readily observed when a concentration slug in a plug flow without molecular diffusion is simulated by numerical methods. The discontinuities in concentration at the front and rear of the slug are not preserved as rounded shoulders, and spreading tails quickly appear. To deal with this numerical dispersion artifact, Boris and Book (10-12) developed the *Flux-Corrected Transport Algorithm* (FCTA) which we have applied to the dispersion problem in this work. The advantages of the FCTA over other well-known numerical methods (e.g., Lax-Wendroff and Crank-Nicholson) for convection-dominated transport problems have been demonstrated by Boris and Book (10). Complete details of the FCTA application to the dispersion problem of the preceding section are given elsewhere (13).

Briefly, the FCTA proceeds in two stages. In Stage I the spatial derivatives in Eq. (3) are approximated by second-order central differences (14), the time derivative is approximated by a first-order forward difference, and a standard explicit estimate of the concentration field at the next time step is obtained. This estimate is “corrected” by addition of an artificial axial diffusion term. In Stage II an “antidiffusion” correction, which depends in a complex way on the axial concentration gradient obtained from Stage I, is imposed. This two-stage sequence is repeated at each time step for calculation of the concentration at all interior grid points.

For our dispersion problem, stable boundary values were obtained by simple second-order backward difference approximations to the zero flux conditions at the tube center and wall. A tube of finite length, and thus computations of reasonable time, were realized by approximating the axial partial derivative in Eq. (3) with a first-order backward difference at the last axial grid location. A second-order central difference was employed for this derivative at all other axial grid locations. Finally, a fourth-order Simpson’s rule approximation served to calculate the area averaged mean concentration (Eq. 5).

The accuracy of the FCTA for simulation of slug dispersion at short times (convection predominating) may be inferred from Boris and Book (10). For long times, Taylor's analytical solution (1) is available for comparison with the FCTA solution. This comparison is shown (Fig. 9), and quite satisfactory agreement is apparent. For intermediate times we expect the FCTA to provide an accurate picture of the dispersion process as it evolves toward the Taylor dispersion limit.

## NUMERICAL RESULTS

All of the results presented in this section were obtained with the following finite difference mesh parameters:  $\Delta t^* = .0001$ ,  $\Delta Z^* = .00104$ ,  $\Delta r^* = .0333$ . The initial slug length was fixed at  $Z_s^* = 8(\Delta Z^*)$  in each case. It was observed that variation of the initial slug length did not affect the qualitative features of the dispersion process which are discussed below.

Elution curves based on the area averaged mean concentration are displayed in Figs. 1, 3, 5, 7, and 9 for five axial locations ranging from convection dominated dispersion ( $Z^* = 0.0203$ ) to Taylor dispersion ( $Z^* = 0.813$ ). A companion figure is presented for each of the first four axial locations (Figs. 2, 4, 6, and 8) which contains elution curves based on point concentrations at three radial positions ( $r^* = 0.0, 0.7, 1.0$ ).

Figure 1 shows the mean elution curve at an early time (short axial distance,  $Z^* = 0.0203$ ) and compares it to Taylor's pure convection analytical solution (1). The elution time for the sharp mean concentration peak ( $t^* = t_1$ ) nearly coincides with the elution time for the point concentration at the center of the tube (cf. Fig. 2). Clearly the predominance of convection in the central region of the tube is responsible for the sharp peak in the mean elution curve. Figure 2 displays point elution peaks of more gradual rise and greater dispersion at lower velocity radial positions. These peaks indicate a stronger diffusional influence in the tube wall region which also reveals itself as a gentle shoulder on the tail side of the mean elution curve (Fig. 1).

At somewhat greater axial distance ( $Z^* = 0.1$ , Fig. 3), the mean elution curve is distinguished by a rather surprising double peak. The sharp first peak is again a manifestation of convection domination in the central region of the tube. The gentle second peak is the evolution of the diffusion shoulder which appeared in Fig. 1. The strong spatial segregation of convection and diffusion regimes which produces the double peak in the mean elution curve is clearly exposed in Fig. 4 which shows nearly identical broad elution curves at  $r^* = 0.7$  and  $1.0$  of character quite distinct from the sharp curve at  $r^* = 0.0$ .

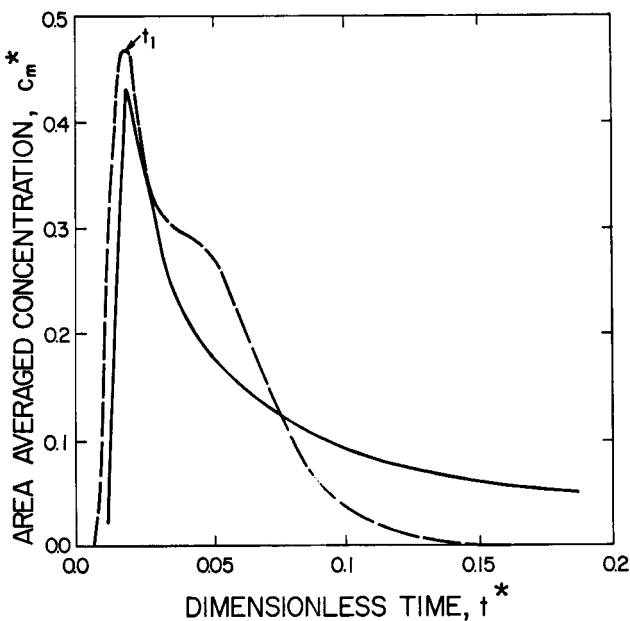


FIG. 1. Mean breakthrough curve at  $Z^* = 0.0203$ . (—) Pure convection solution, (---) numerical solution,  $t_1 = 0.018$ .

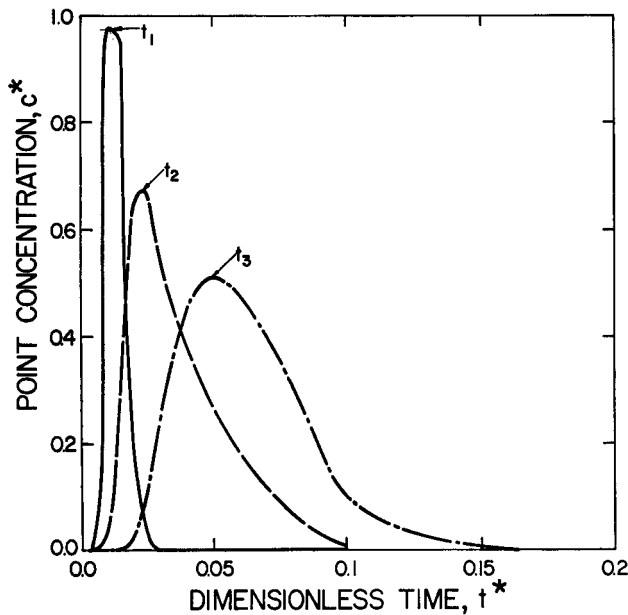


FIG. 2. Internal breakthrough curves at  $Z^* = 0.0203$ . (—)  $r^* = 0.0$ , (---)  $r^* = 0.7$ , (---)  $r^* = 1.0$ ,  $t_1 = 0.013$ ,  $t_2 = 0.024$ ,  $t_3 = 0.05$ .

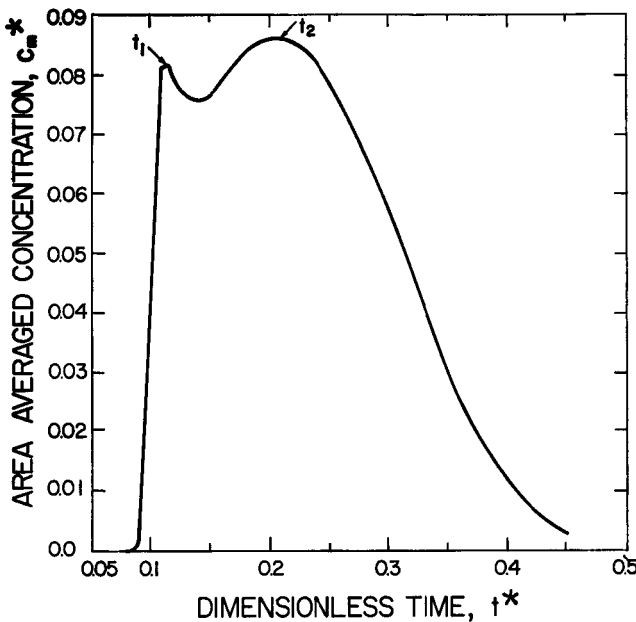


FIG. 3. Mean breakthrough curve at  $Z^* = 0.10$ .  $t_1 = 0.113$ ,  $t_2 = 0.210$ .

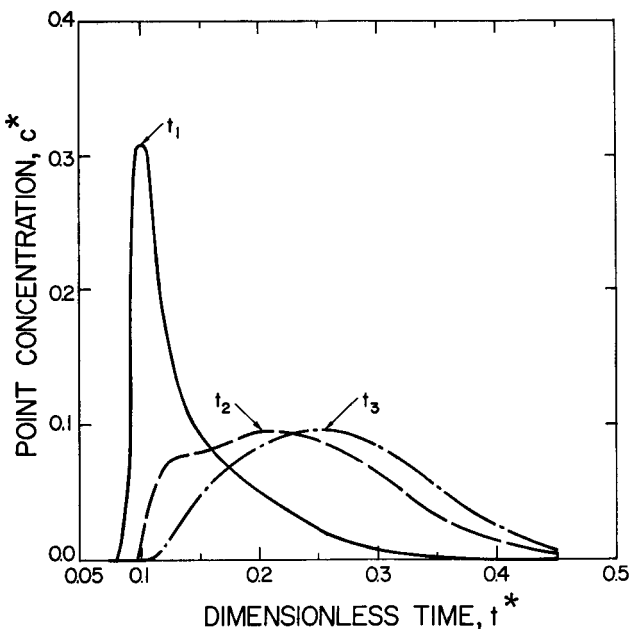


FIG. 4. Internal breakthrough curves at  $Z^* = 0.10$ . (—)  $r^* = 0.0$ , (---)  $r^* = 0.7$ , (- -)  $r^* = 1.0$ ,  $t_1 = 0.105$ ,  $t_2 = 0.210$ ,  $t_3 = 0.250$ .

Further down the tube ( $Z^* = 0.124$ , Fig. 5), the broad diffusion peak becomes the dominant feature of the mean elution curve with the last remnant of a convection regime appearing as a sharp shoulder on the rise of the curve. The elution curve at the center of the tube is still sharply peaked (Fig. 6) and not strongly influenced by diffusion.

At  $Z^* = 0.294$  (Fig. 7) the mean elution curve is single peaked without shoulders and reasonably well approximated by Taylor's analytical solution (1). The point elution curves (Fig. 8) are nearly coincident and the influence of diffusion has now strongly affected the central region of the tube. By the time  $Z^* = 0.813$  (Fig. 9) is reached, fully developed Taylor dispersion is obtained and, although not shown, the point elution curves at all radial positions are indistinguishable.

The asymptotic development of Taylor dispersion is displayed quantitatively in Fig. 10 which is a parametric plot of the peak elution times [ $t_p(r^*)$ ], normalized by the mean elution time in Taylor dispersion ( $t_m$ ), as a function of axial position. The point elution curves are coherent in the Taylor dispersion limit which is, for practical purposes, reached at  $Z^* = 0.8$ .

## DISCUSSION

Caro (15) measured breakthrough curves for the laminar dispersion of red dye in water flowing through curved and straight tubes. Double peaks were reported for both geometries. Although Caro attributed the behavior to secondary flow effects in the curved tube, he offered no explanation for the double peaks obtained in the straight tube.

More convincing experimental confirmation of our results has been reported by Liauh (16) who measured the dispersion of sodium polystyrene sulfonate slugs (of various molecular weights and diffusivities) by aqueous  $\text{Na}_2\text{SO}_4$  solvent in laminar flow through a straight tube. In a sequence of experiments (employing an ultraviolet detector at the end of a fixed length of tube) in which the molecular weight of the polymer solute was varied from  $1 \times 10^6$  to  $4 \times 10^3$ , the observed breakthrough curves were transformed from single peak through double peak and back again to single peak. These qualitative changes are quite in accord with our numerical results (cf. Figs. 1, 3, 5, 7, and 9). Unfortunately, a more quantitative comparison between theory and experiment is not possible because the sodium polystyrene sulfonate diffusivities are difficult to measure and depend markedly on concentration (17).

In conclusion, we feel that the detailed numerical work presented in this paper fills a theoretical void in the understanding of laminar dispersion. It bridges the gap between convective and Taylor dispersion and in the

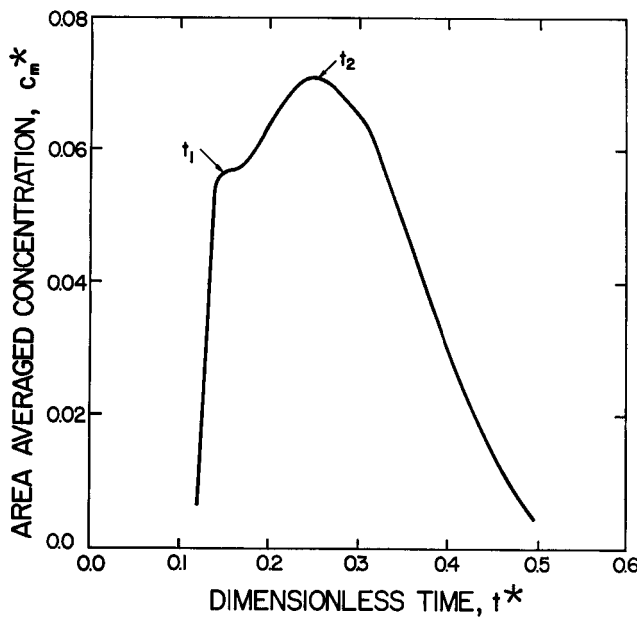


FIG. 5. Mean breakthrough curve at  $Z^* = 0.124$ .  $t_1 = 0.124$ ,  $t_2 = 0.250$ .

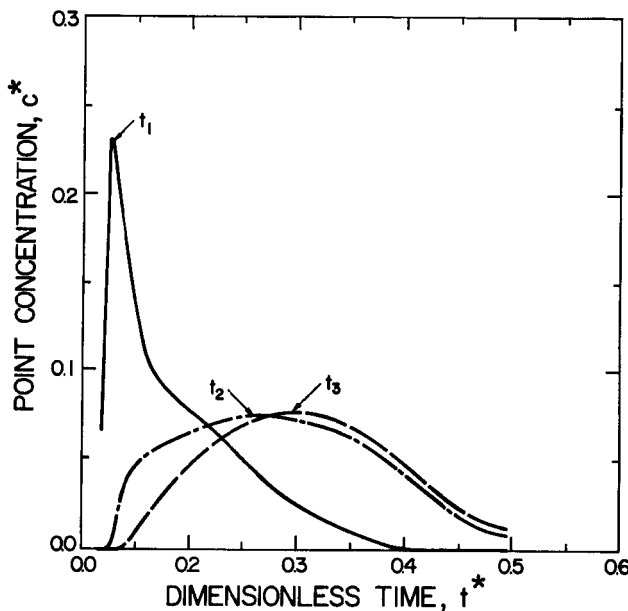


FIG. 6. Internal breakthrough curves at  $Z^* = 0.124$ . (—)  $r^* = 0.0$ , (---)  $r^* = 0.7$ , (- · -)  $r^* = 1.0$ ,  $t_1 = 0.130$ ,  $t_2 = 0.265$ ,  $t_3 = 0.300$ .

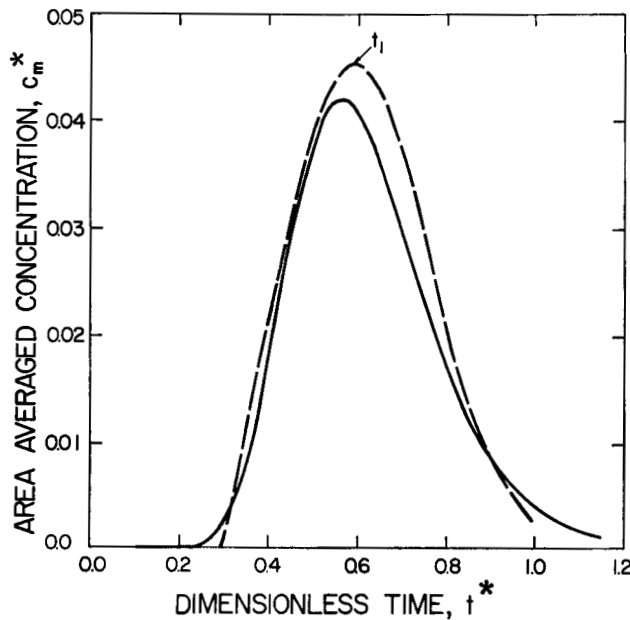


FIG. 7. Mean breakthrough curve at  $Z^* = 0.294$ . (—) Taylor's analytic solution ( $I$ ), (- -) numerical solution,  $t_1 = 0.585$ .

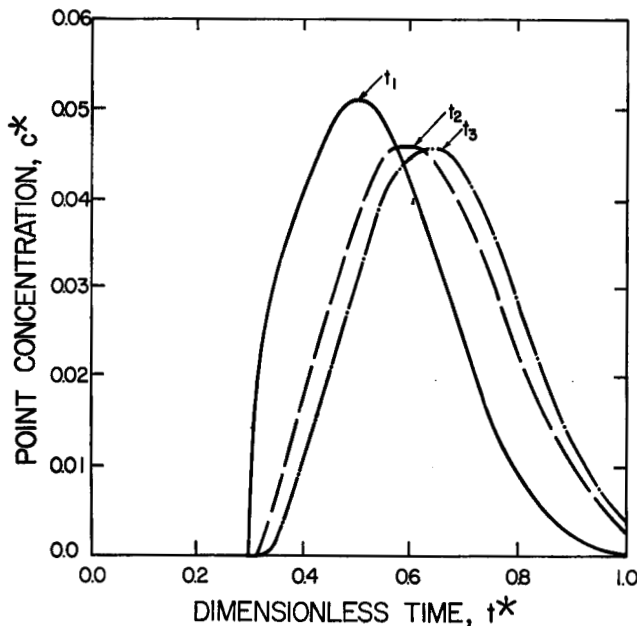


FIG. 8. Internal breakthrough curves at  $Z^* = 0.294$ . (—)  $r^* = 0.0$ , (- -)  $r^* = 0.7$ , (- - -)  $r^* = 1.0$ ,  $t_1 = 0.500$ ,  $t_2 = 0.600$ ,  $t_3 = 0.630$ .

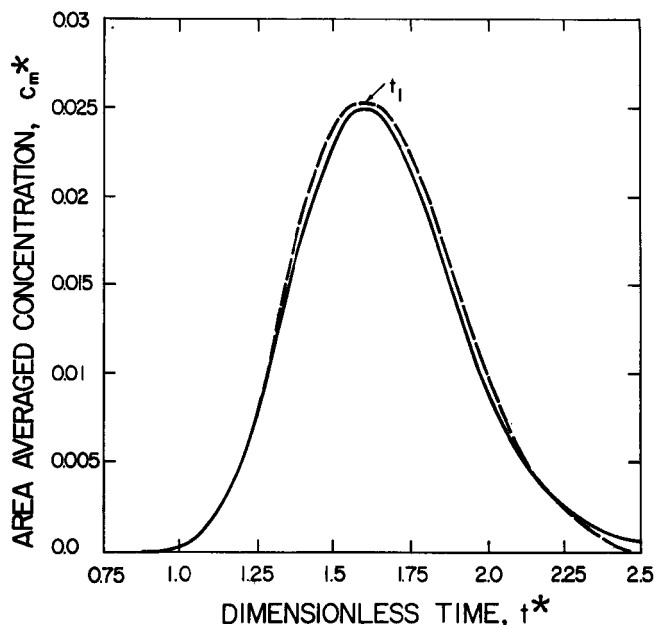


FIG. 9. Mean breakthrough curve at  $Z^* = 0.813$ . (—) Taylor's analytical solution ( $I$ ), (---) numerical solution,  $t_1 = 1.60$ .

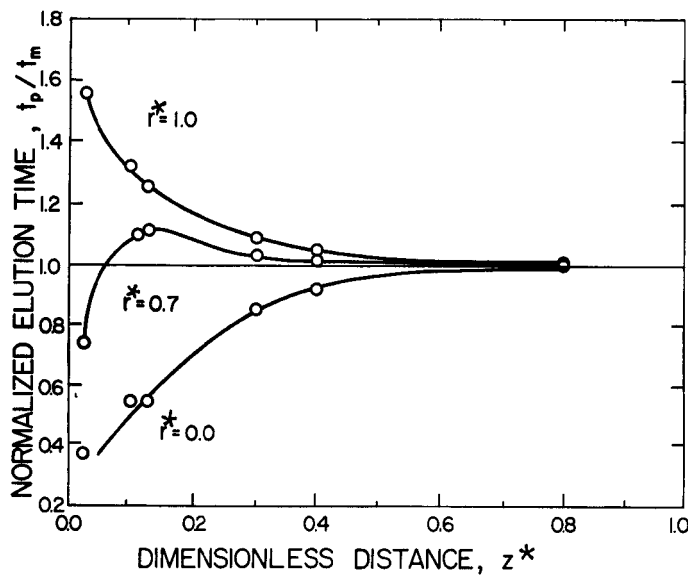


FIG. 10. Normalized elution times for internal breakthrough curves.

process reveals the rather surprising double peak phenomena which we have discussed at length.

### NOTE ON RECENT WORK

Since this paper was accepted for publication, a paper by Golay and Atwood (18) has come to our attention. These authors have observed double peaking phenomena in pulse dispersion experiments in laminar tube flow employing sodium benzoate in water. Our Figs. 1, 3, and 5 are strikingly similar to the experimental breakthrough curves shown in their Fig. 10. Golay and Atwood have also performed numerical calculations by methods quite distinct from ours, and have predicted double peak breakthrough curves.

### SYMBOLS

$c$	concentration
$c_0$	initial slug concentration
$c^*$	dimensionless concentration
$c_m^*$	dimensionless area averaged mean concentration
$D$	molecular diffusion coefficient
$r$	radial coordinate
$r^*$	dimensionless radial coordinate
$R$	tube radius
$t$	time
$t^*$	dimensionless time
$t_m$	elution time in Taylor dispersion
$t_p$	peak elution time for internal breakthrough curves
$u_0$	centerline velocity
$Z$	axial coordinate
$Z^*$	dimensionless axial coordinate
$Z_s$	slug length
$Z_s^*$	dimensionless slug length

### REFERENCES

1. G. I. Taylor, *Proc. R. Soc. London*, *A219*, 186 (1953).
2. R. Aris, *Ibid.*, *A235*, 67 (1956).
3. M. N. Gill and R. Sankarasubramanian, *Ibid.*, *A316*, 341 (1970).
4. K. Jayaraj and R. Subramanian, *Sep. Sci. Technol.*, *13*, 791 (1978).
5. P. C. Fife and K. R. K. Nicholes, *Proc. R. Soc. London*, *A344*, 131 (1975).
6. M. J. Lighthill, *J. Inst. Math. Its Appl.*, *2*, 97 (1966).
7. V. Ananthakrishnan, W. N. Gill, and A. J. Barduhn, *AIChE J.*, *11*, 1063 (1965).
8. H. R. Bailey and W. B. Gogarty, *Proc. R. Soc. London*, *A269*, 352 (1962).
9. P. J. Roache, *J. Comput. Phys.*, *10*, 169 (1972).

10. J. P. Boris and D. L. Book, *Ibid.*, 11, 38 (1973).
11. D. L. Book, J. P. Boris, and K. Hain, *Ibid.*, 18, 248 (1975).
12. J. P. Boris and D. L. Book, *Ibid.*, 20, 397 (1976).
13. K. P. Mayock, "Numerical Analysis of Laminar Dispersion in Porous and Non-porous Capillaries," M.S. Thesis, Pennsylvania State University, 1979.
14. W. F. Ames, *Numerical Methods for Partial Differential Equations*, Barnes and Noble, New York, 1969.
15. C. G. Caro, *J. Physiol. (London)*, 185, 501 (1966).
16. W. Liauh, "Mass Transfer in a Laminar Flow Field with Ultrafiltration and Its Application in Polymer Fractionation," Ph.D. Thesis, Pennsylvania State University, 1979.
17. Y. Suzuki, I. Noda, and M. Nagasawa, *J. Polym. Chem.*, 1969 73, 797 (1969).
18. M. J. E. Golay and J. T. Atwood, in *Advances in Chromatography* (A. Zlatkis, ed.), University of Houston Press, Houston, 1979, p. 369.

*Received by editor October 5, 1979*